Proceedings of the 17th World Congress
The International Federation of Automatic Control
Seoul, Korea, July 6-11, 2008

A Multi-Operational-Mode Anti-Sway and Positioning Control for an Industrial Bridge Crane ⋆,⋆⋆

Khalid Sorensen * **Hannas Fisch** ** **Steve Dickerson** ***
William Singhose * **Urs Glauser** **

* *Woodruff School of Mechanical Engineering, Georgia Institute of Technology, Atlanta, GA, 30332 USA (Tel: 404-385-0668; e-mail: Singhose@ Gatech.edu)*
** *Zurich University of Applied Sciences, Winterthur, Switzerland*
*** *CAMotion Inc., Atlanta, GA, 30318 USA (Tel: 404-874-0090; e-mail: Steve.Dickerson@ Camotion.com)*

Abstract: A 30-ton industrial bridge crane located at an aluminum sheet manufacturer has been equipped with a crane manipulation system enabling swing-free motion, disturbance rejection, and precise positioning. Previous investigations of anti-sway, positioning, and crane control have yielded important contributions in these areas. These advancements are combined into the unified crane manipulation system described here. An overview of this system is presented, along with experimental results, and a description of how human operators use the crane.

Keywords: Input Shaping; Command Shaping; Crane Control; Anti-Sway; Feedback Control; Machine Vision.

1. INTRODUCTION

CRANES are used throughout the world in thousands of shipping yards, construction sites, steel mills, warehouses, nuclear power and waste storage facilities, and other industrial complexes. Safe and efficient motion of these structures is an important contributor to industrial productivity.

An important property of cranes that can adversely affect safe and efficient motion is the tendency for a crane payload to swing. External disturbances, such as wind, or commanded motion can cause significant payload swing. Payload swing makes precise positioning time consuming for a human operator; furthermore, when the payload or surrounding obstacles are of a hazardous or fragile nature, payload swing may present a safety hazard.

The broad usage of cranes, coupled with the need to reduce undesired oscillation, has motivated a large amount of research. Significant advancements have been made in the areas of 1) motion-induced oscillation reduction, 2) disturbance rejection, 3) positioning capability, 4) payload swing detection, and 5) operator interface design. Advancements from each of these areas have been combined into a unified crane manipulation system (CMS). The utility of the CMS is that it provides operators with a means for generating safe and efficient swing-free motion, and the capability for precise positioning.

This paper describes the components of the CMS, and the implementation of this system on a 30-ton industrial bridge crane. This crane is located at Logan Aluminum, a leading manufacturer of aluminum sheet products.

In Section 2, a description of the Logan crane and its dynamic behavior is presented. Section 3 provides an overview of the CMS and how this system is integrated into the Logan crane. Results of performance experiments conducted on the CMS-equipped Logan crane are presented in Section 4.

2. SYSTEM DESCRIPTION

Figure 1 shows a photograph of the 30-ton Logan crane. The trolley traverses along the bridge, which spans a distance of approximately 30 meters. Likewise, the bridge can traverse along stationary rails for a distance of approximately 50 meters. The hook is suspended beneath the trolley. During operation, the suspension cable length varies between 3 and 10 meters.

The bridge is equipped with two 7.5-kilowatt (10 - horsepower) 480-volt AC induction motors. Similarly, the trolley is equipped with two 3.75-kilowatt (5 - horsepower) 480-volt AC induction motors. The motors are controlled by Magnetek Impulse P^3 vector drives. This equipment permits continuously variable velocity control. Additionally, the drives are parameterizable. The maximum permissible velocity and acceleration limits have been programmed to be $0.75m/s$ and $0.75m/s^2$, respectively.

⋆ This work was supported by CAMotion Inc. Logan Aluminum, and Siemens Energy & Automation.
⋆⋆**Patent Notice:** The control methods described in this paper are protected by the World Intellectual Property Organization (WO 2006/115912 A2). Commercial use of these methods requires written permission from CAMotion Inc. and the Georgia Institute of Technology.

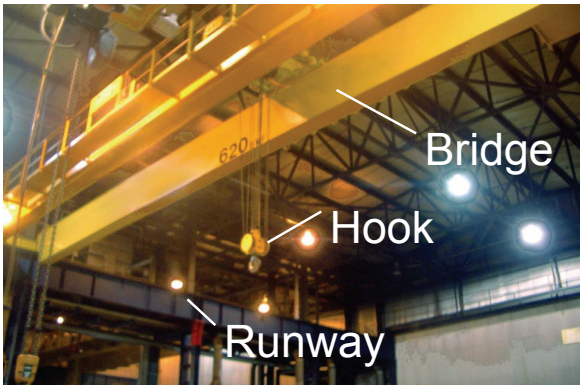

(a) Bridge, hook, and runway.

(b) Closeup of trolley.

Fig. 1. 30-ton bridge crane at Logan Aluminum.

Prior to installation of the CMS, an operator actuated the crane by issuing commands from a lever interface directly to the crane drives. A model of this actuation process is illustrated with the block diagram of Fig. 2. DM, represents the behavior of the system's vector *drives* and AC induction *motors*. This plant accepts reference velocity commands, V_r, issued to the crane by a human operator, and converts these signals to the actual velocity of the overhead trolley, V_t. Motion of the trolley causes the hook and attached payload to swing with cable angle, θ. This behavior is represented by the block, G.

2.1 Dynamic Model of Industrial Cranes

The behavior of AC induction motors and vector drives is nonlinear. However, this behavior can be accurately modeled by combining several simpler components [Sorensen, 2005]. The DM block of Fig. 2 is expanded in Fig. 3 to reveal such a model.

The model is comprised of four elements: a saturator, a switch, a rate limiter, and a heavily damped second-order plant, H. The saturation element truncates excessive velocity commands to the crane, while the rate limiter places upper and lower bounds on the acceleration of the crane. H serves to mimic the smoothing behavior of the drives and motors. The function of the switching element is to pass the reference signal, $\widetilde{V}_r$, to the rate-limiting block.

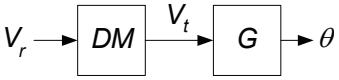

Fig. 2. Crane actuation block diagram.

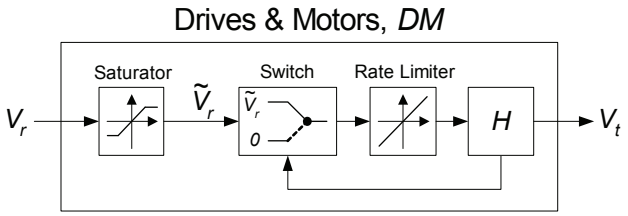

Fig. 3. Expanded view of the drives & motors model block.

However, when transitional velocity commands are issued to the crane, the switch temporarily sends a signal of zero. Transitional velocity commands are those commands that change the direction of travel of the crane (forward to reverse or vise versa). This type of behavior depends on $\widetilde{V}_r$ and V_t, and can be described with the following switching rules:

$$Switch = \begin{cases} \widetilde{V}_r, & \text{Sign}(\widetilde{V}_r) = \text{Sign}(V_t), \\ \widetilde{V}_r, & |V_t| \leq X, \\ 0 & \text{otherwise.} \end{cases} \quad (1)$$

This model may be used to represent the behavior of the Logan crane drives and motors by properly selecting the five parameters associated with the model: p - the saturation threshold, X - the switching threshold, m - the maximum slope of the rate limiter, ζ_H - the damping ratio of H, and ω_{nH} - the natural frequency of H. For the Logan crane, these parameters were estimated to be $0.75m/s$, $0.038m/s$, $0.63m/s^2$, 0.75, and $3.7rad/s$, respectively. Figure 4 compares the response of the model and the response of the actual system to several velocity commands.

When the motors move the crane, oscillations are induced into the hook. As previously illustrated in Fig. 2, the angular response of the hook to motion of the trolley is modeled by the plant, G. The oscillatory behavior of the hook can be represented by a linear transfer function [Sorensen et al., 2007a]:

$$G = \frac{\theta(s)}{V_t(s)} = \frac{(-\omega_n^2/g)s}{s^2 + 2\zeta\omega_n s + \omega_n^2}. \quad (2)$$

For the Logan crane, the damping ratio, ζ, is approximately 0.01. The natural frequency, ω_n, is a function of the cable suspension length, L, and the acceleration due to gravity, g:

$$\omega_n = \sqrt{g/L}. \quad (3)$$

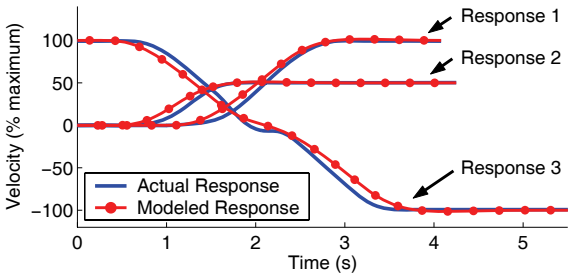

Fig. 4. Comparison of the actual and modeled responses of the drives & motors to different velocity commands. (1) Response to a step of 100% velocity. (2) Response to a step of 50% velocity. (3) Response to a step from 100% velocity to -100% velocity.

3. INTEGRATION OF THE CMS

The crane described in Section 2 has been augmented with the CMS. A topological illustration of the CMS-equipped crane is shown in Fig. 5. This figure depicts the elements that comprise the CMS:

- A control architecture for enabling swing-free motion and precise payload positioning.
- A visual human-machine interface for aiding precise positioning of the crane. This interface is implemented on a touch screen monitor.
- A joystick interface for simplifying gross motion tasks.
- A standard lever interface.
- A machine vision system for sensing hook swing.
- Laser range sensors for measuring crane position.

The principal element of the CMS is the anti-sway and positioning control. This component accepts information from the other CMS elements: motion commands from the three interface devices, crane position information from the laser range sensors, and hook displacement information from the machine vision system. The information from these elements is used by the control to produce low-sway velocity commands, which are issued to the crane drives. The following subsections provide greater detail about each element of the CMS.

3.1 Human-Machine Interface

Prior to installation of the CMS onto the Logan crane, operators commanded crane motion by using a three-lever interface. This device permits the bridge, trolley, and hook to be commanded independently from each other by their respective actuation levers. Two additional interface devices were installed with the CMS: a joystick interface, and a visual touch-screen interface.

The motivation for implementing these devices was rooted in improving the way operators control the crane. The visual interface permits simplified positioning control, while the joystick permits simplified velocity control.

Simplified Positioning. In many applications, precise and repetitive payload positioning is required. The visual interface is a real-time graphical representation of the crane and crane workspace that permits operators to store desired payload destinations, and also command the crane to travel to these locations [Suter et al., 2007, Sorensen et al., 2007b]. To store a payload destination for future use, an operator must first manually position the crane in this location. Then, the coordinates corresponding the crane's position can be automatically stored into the visual interface. A target image represents the location on the touch screen. Operators specify a desired hook destination by touching a stored target that is displayed in the graphical workspace image. Once the operator specifies the desired destination, the feedback control system automatically drives the crane to the specified location without payload sway.

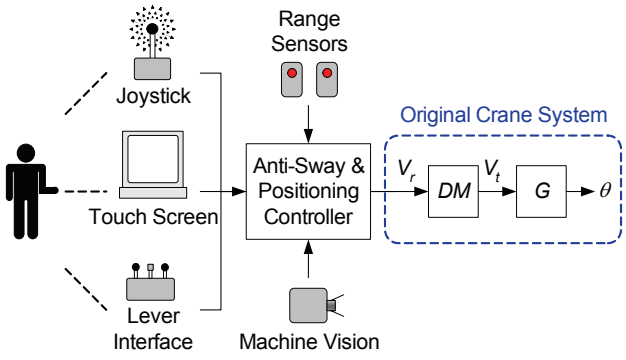

Fig. 5. Components of the CMS integrated into a crane system.

Figure 6 is a screen-shot of the visual interface. In region *A*, the operator can store and specify hook destinations. Region *B* displays various system indicators, such as anti-sway activity, system errors, and operation mode. Region *C* displays actual and desired crane position information.

For precise positioning applications, the visual interface yields significant efficiency advantages over traditional manual control [Sorensen et al., 2007b]. This is because operators using the interface can automatically position the crane at a desired location in a nearly time-optimal and swing-free manner. Manual positioning is more difficult. Operators must have extensive training. Often, the structures are moved very slowly to ensure accurate and safe positioning.

A visual interface, similar to the one described here, was installed on a 10-ton industrial bridge crane located at the Georgia Institute of Technology. Operator studies conducted on this crane revealed that operators using the visual interface completed positioning tasks 5% to 45% more quickly than with manual control [Sorensen et al., 2007b].

In addition to positioning simplicity, there are other benefits to using the visual interface. These benefits are related to the cognitive processes of the human operator. The type of gesture-based control provided by the visual interface utilizes intuition-based behavior [Frigola et al., 2003, Amat et al., 2004], which is less complex and requires less cognitive resource use than manual positioning. As discussed in [Stahre, 1995], a tremendous benefit of "shifting" operator actions toward intuition-based behavior is that more

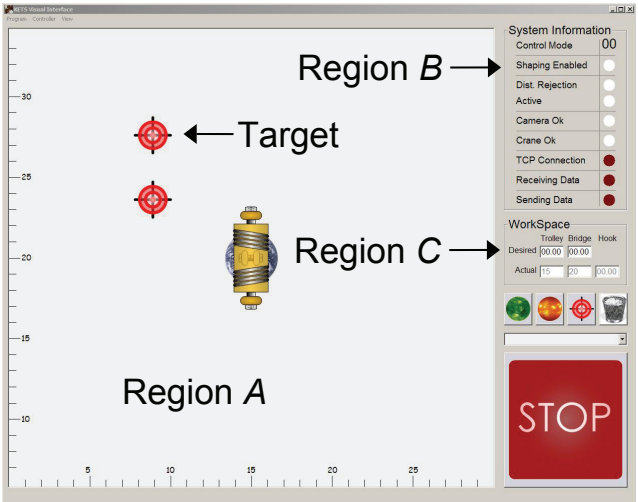

Fig. 6. Screen shot of the Logan crane visual interface.

mental resources of the operator are free to analyze new situations and monitor existing states of the system.

Simplified Velocity Control. Whereas the visual interface facilitates automatic crane motion, the lever and joystick interfaces can be used for manual motion tasks. Generally, the joystick interface permits these types of tasks to be completed more efficiently than the lever interface [Sorensen et al., 2007b].

When an operator attempts to command crane motion using a lever interface, he or she mentally accomplishes several steps. First, the desired trajectory of the hook and payload is decoupled into the kinematic components corresponding to the different modes of actuation (i.e. forward-reverse, left-right, up-down). Second, the decoupled trajectories are mentally mapped to the corresponding actuating levers. Finally, the operator attempts to physically depress the correct combination of levers so that the crane traverses along the desired trajectory. For efficient motion, generally two levers must be controlled simultaneously by the operator. Because this is difficult, operators often manipulate the crane along less efficient trajectories that require motion in only one actuation direction at a time.

To manipulate the crane with the joystick, operators point the joystick handle in a desired direction with variable displacement. The direction and displacement of the joystick handle correspond to the direction and velocity of crane travel. This mode of manual control can facilitate more efficient crane motion than the lever interface. This is because it is easier for an operator using the joystick to simultaneously actuate the crane in both the bridge and trolley directions.

3.2 Sensory Information

Machine Vision System. Sensory information about hook swing is obtained by using a Siemens 720-series vision system. This camera is a stand-alone image sensor with on-board image acquisition, processing, and communication capabilities. The vision system is mounted on the trolley, near the fulcrum of the hook suspension cables, and oriented to view the hook and surrounding workspace. In this downward-looking configuration, the top of the crane hook is always within the camera field-of-view, as shown in Fig. 7.

To facilitate reliable hook tracking, a light-emitting-diode (LED) array was installed. When the vision system acquires an image, the LED array simultaneously pulses (similar to a flash bulb on a camera). Two fiducial markers made of retro-reflective material, and mounted to the top of the hook, reflect the pulsed light back to the camera lens. By so doing, the fiducial markers are easily discernable from other features in the image. A close up view of the fiducial markers is shown in the sub photograph of Fig. 7.

The camera acquires an image every $70ms$. A program within the camera processes the image to obtain coordinate information about the fiducial markers. This information is subsequently communicated to the anti-sway and positioning controller.

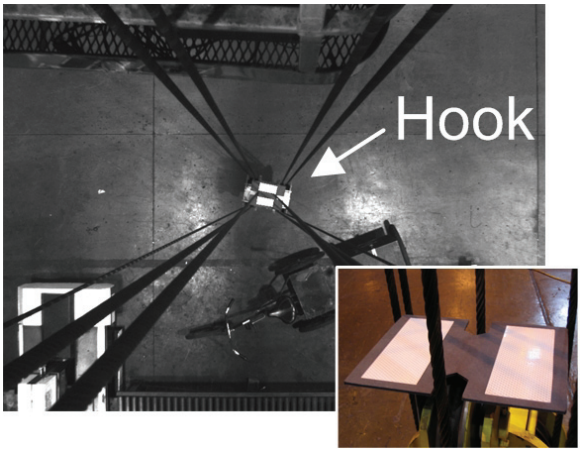

Fig. 7. Image captured and processed by the machine vision system (large photo). Close up photograph of the fiducials mounted on the hook (sub photo).

Laser Range Sensors. Absolute bridge and trolley positions are obtained by using two Banner LT3-series laser range sensors. These position sensors have a range of $50m$ and a resolution of approximately $1.2cm$ at this distance. Both sensors are mounted on the bridge. One is oriented to detect the position of the trolley along the bridge. The other is oriented to detect the position of the bridge along the stationary runways.

3.3 Anti-Sway & Positioning Control

A block diagram of the anti-sway and positioning control is shown in Fig. 8. This block diagram depicts a control architecture where the original crane system is integrated into a two-loop feedback structure. The control generates reference velocity commands that, when issued to the nonlinear drive and motors plant, DM, achieve three desirable results in the payload: 1) precise positioning capability, 2) motion-induced oscillation suppression, and 3) disturbance rejection.

In the subsections that follow, brief descriptions of the control elements that enable these result to be achieved are provided. Because a thorough description of this control and its stability is beyond the scope of this paper, the reader interested in the development of this control and the results of rigorous stability analyses should refer to [Sorensen, 2005, Sorensen et al., 2007a, Sorensen and Singhose, 2007].

Motion-Induced Oscillation Suppression. A successful approach to suppressing motion-induced oscillation is to generate a command that causes a system to cancel out its own oscillation. One such technique, called *input shaping*, is implemented by convolving a reference command with a sequence of impulses called an *input shaper* [Smith, 1957, Singer and Seering, 1990]. The convolution product, instead of the original reference command is then issued to the plant. For correctly designed input shapers, a linear system will exhibit zero residual oscillation in response to the modified command. This scenario is illustrated in Fig. 9(a). The reference command (in this case a step) is modified by the two-impulse input shaper. The impulse times and impulse amplitudes of the shaper have been properly selected to negate the oscillatory dynamics of H.

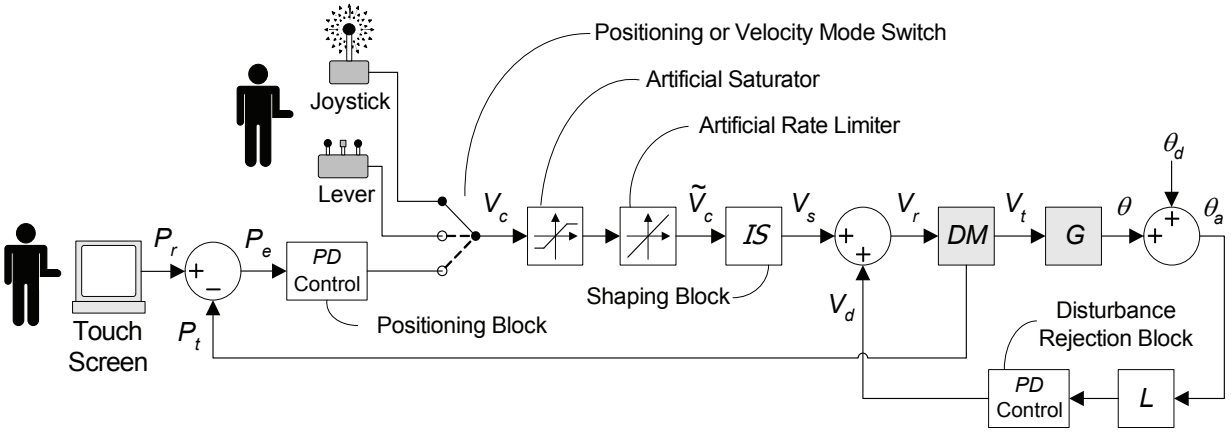

Fig. 8. Anti-sway & positioning controller.

When the shaped command actuates H, the result is zero residual oscillation. A block diagram representing a general input shaping process is shown in Fig. 9(b). IS is the input shaper and H is the linear plant.

This type of motion-induced oscillation suppression is integrated into the CMS control structure by incorporating an input shaper into the signal path. In Fig. 8, the input shaper is represented by the block labeled IS. This shaper is designed to negate the oscillatory dynamics of the closed-loop transfer function formed by the disturbance rejection feedback loop. The input shaper accepts commanded velocity signals, V_c, from one of three elements. If the crane is being manually manipulated, then signals from the joystick or lever interface are issued to the input shaper. If the crane is being automatically positioned through the use of the touchscreen, then signals from a positioning control block are issued to the shaper. The shaped commands, V_s, are then used as reference commands for the disturbance rejection loop.

While input shaping works effectively for linear systems, the nonlinear elements contained in the drives and motors, DM, can significantly reduce the capacity of the shaped commands to eliminate oscillation [Lawrence et al., 2004, 2005, Sorensen and Singhose, 2007]. A strategy to mitigate the detrimental effects of saturation and rate limiting within the DM block was presented in [Sorensen and Singhose, 2007]. An artificial saturation element, and an artificial rate limiting element may be incorporated into the signal path such that these elements filter reference commands before they are modified by the input shaper. By so doing, the shaped command generated by the input shaper will not be corrupted by the saturation and rate limit elements contained in the drives and motors. The saturation and rate limiting parameters of the artificial elements must be equal to, or more conservative than, the actual saturation and rate limiting parameters.

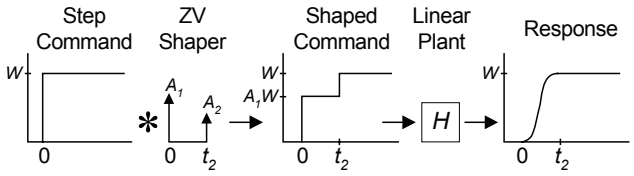

(a) Shaped command actuating a linear plant.

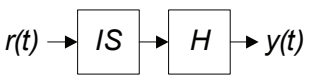

(b) Input shaping block diagram.

Fig. 9. Input shaping process.

Precise Payload Positioning. When an operator controls the crane by using the visual interface, position reference commands are issued to the CMS control. Given that a payload eventually comes to rest directly beneath the overhead support unit, final positioning of the trolley is equivalent to final positioning of the payload. Therefore, precise payload positioning is accomplished by using position information from the laser range sensors to control the position of the trolley. P_r, P_t, and P_e are the reference trolley position, actual trolley position, and positioning error, respectively.

In response to the positioning error, a proportional-derivative (PD) control block generates a velocity signal that attempts to drive the crane toward the desired location. If this signal were issued *directly* to the drives and motors, then the objective of trolley positioning would be accomplished, but, noticeable hook swing would be exhibited. However, because the input shaper filters these commands, the dual objective of driving the crane toward a desired position, while also preventing motion-induced oscillation is achieved.

The use of input shapers within feedback loops is a non-conventional control architecture. Nevertheless, a significant body of literature exists that addresses the stability of these types of systems [Zuo et al., 1995, Kapila et al., 2000, Staehlin and Singh, 2003, Huey and Singhose, 2005]. For the CMS control, stable PD control gains that achieved desirable system performance were obtained by using a root locus approximation technique presented in [Huey and Singhose, 2005]. This root locus technique neglects the nonlinear elements within the control structure, and therefore, does not guarantee the stability of the nonlinear system. It does, however, serve to provide insight into the dynamics of the shaper-in-the-loop system, and reveals the anticipated behavior when the system operates within its linear region. The PD control gains obtained from the root

locus approximation technique were rigorously verified on a nonlinear model of the system by using numerical methods presented in [Sorensen et al., 2007a].

Disturbance Rejection. While the primary source of cable sway is commanded motion, secondary sources of oscillation, such as external disturbances, or unmodeled dynamics also contribute to undesired hook swing. These types of disturbances may be modeled as inducing a disruptive angle, θ_d, that is summed with the undisturbed angle, θ, to produce the actual cable angle, θ_a.

Disturbance rejection is accomplished by making use of the machine vision system to provide sensory feedback of the actual cable angle, θ_a. For small angles, the horizontal displacement of the hook from the vertical at-rest position can be reasonably estimated by $L\theta_a$. This quantity is utilized in a PD block, which generates corrective velocity commands to damp out the disruptive oscillations. These signals are added to the shaped velocity signals, V_s, obtained from the input shaper. The combined signal is then issued to the system drives.

Although the drives and motors contain nonlinear elements, these components do operate within their linear regions frequently. Therefore, during these periods of time, superposition holds. Thus, because the signal, V_s continually drives the crane toward a desired set point, and the signal, V_d, attempts to damp out oscillation, the CMS control will achieve the dual objectives of positioning and disturbance rejection. Furthermore, because V_s is an input-shaped command, motion-induced hook swing will be reduced. In this way, the CMS control eliminates motion-induced oscillation, rejects disturbances, and enables precise positioning of the payload.

3.4 Beneficial Attributes of Combining Input Shaping with Feedback Control

The control architecture presented in the previous subsection allocates the task of motion-induced oscillation suppression to the input shaping filter. Disturbance-induced oscillation suppression is achieved through feedback control. While feedback *alone* could suppress both motion and disturbance-induced payload swing, beneficial system behavior is exhibited when these tasks are separated [Muenchhof and Singh, 2002, Kenison and Singhose, 2002].

Input shaping reduces motion-induced oscillation in an *anticipatory* manner, as opposed to the *reactive* manner of feedback control. Oscillation suppression is accomplished with the *reference* signal that anticipates the oscillation before it occurs, rather than with a *correcting* signal that attempts to restore deviations back to a reference signal. In the context of crane control, this means that motion-induced oscillation can usually be suppressed within one-half period of oscillation when using input shaping. To achieve similar performance with feedback control, aggressive gains must be used, which results in higher actuator effort, and greater command distortion than when using input shaping.

Another beneficial consequence of allocating motion-induced oscillation suppression to an input shaping filter is related to multi-mode cable sway. For some payload and rigging configurations, cranes can exhibit "double-pendulum" oscillatory dynamics [Singhose et al., In Press]. In such cases, aggressive disturbance rejection feedback gains will cause the nonlinear drives and motors to exhibit limit cycling. By utilizing input shaping, motion-induced oscillation suppression of the multi-mode system can be quickly suppressed without aggressive control gains.

4. CMS PERFORMANCE EVALUATION

The anti-sway and positioning capabilities of the CMS-equipped Logan crane were rigorously tested. Section 4.1 discusses motion-induced oscillation suppression. Section 4.2 discusses disturbance rejection. Finally, Section 4.3 discusses positioning.

4.1 Motion-Induced Oscillation Suppression

To evaluate the capabilities of the CMS to suppress motion-induced oscillation, the crane was driven both with and without the CMS enabled. In the first set of such tests, the lever interface was used to issue a step command in velocity to the bridge. The velocity response of the bridge to this command is shown with the solid line in Fig. 10(a). The oscillatory response of the hook to the bridge motion is shown with the solid line of Fig. 10(b). The same test was conducted when the CMS was enabled. These results are shown with the dotted lines of Fig 10. The bridge exhibits a noticeably different motion profile that causes much less hook swing.

Similar results were obtained when these tests were repeated in the trolley direction, and simultaneously in the trolley and bridge directions. The bar graph of Fig. 11 summarizes the swing amplitude results from each of these tests.

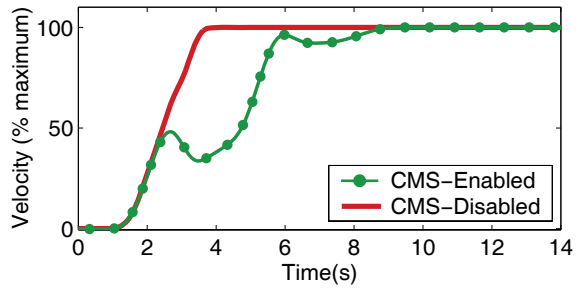

(a) Velocity commands.

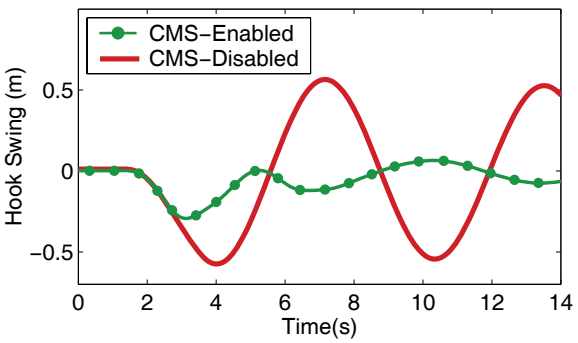

(b) Hook swing.

Fig. 10. Motion-induced oscillation suppression with and without the CMS enabled.

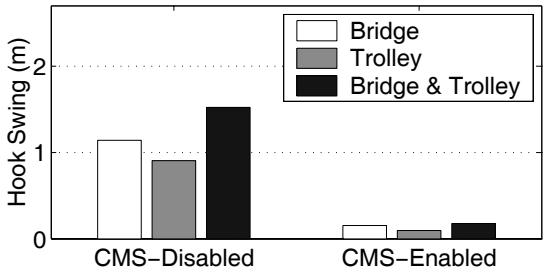

Fig. 11. Residual hook swing amplitude after a step velocity command was issued to the crane.

Another set of tests were conducted where a pulse in velocity (instead of a step) was issued to the crane. For each of these tests, the lever interface was used to quickly accelerate the crane to maximum velocity. After the crane had been traveling at maximum velocity for approximately two seconds, the crane was quickly decelerated to a full stop. The swing amplitude results of these tests are summarized in the bar graph of Fig. 12.

The results summarized in Figs. 11 and 12 demonstrate that the CMS-equipped crane can reduce motion-induced oscillation by roughly 90%.

4.2 Disturbance Rejection

The disturbance rejection capabilities of the CMS were evaluated by imparting an initial hook swing to the system while the CMS was deactivated. Then, the CMS was activated while crane position and hook position data were being recorded. This experiment was repeated at several different suspension cable lengths ranging from $10m$ to $3m$.

A typical system response to this experiment is shown in Fig. 13. The bridge position is shown with the solid line and the payload position is shown with the dotted line. The CMS was activated at approximately time $t = 6s$. The hook oscillations were mostly damped out by time $t = 17s$, a time duration of approximately two oscillation periods.

4.3 Positioning Capabilities

The positioning capabilities of the CMS were evaluated by issuing several reference positions to the crane. The automatic control attempted to drive the crane to the desired positions while limiting motion-induced and disturbance-induced oscillations. The response of the crane to a typical

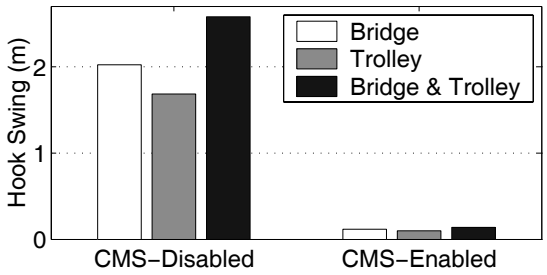

Fig. 12. Residual hook swing amplitude after a pulse velocity command was issued to the crane.

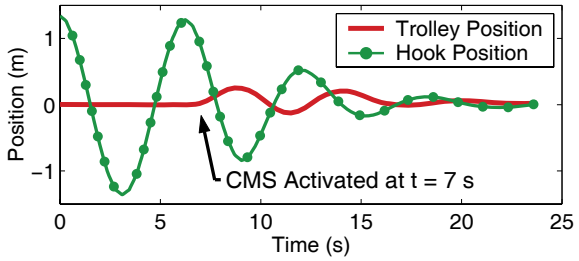

Fig. 13. Cancelation of disturbance-induced oscillations.

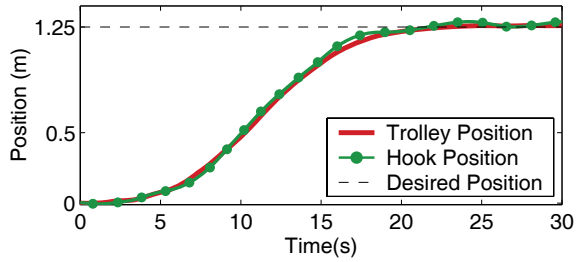

Fig. 14. CMS-enabled trolley response to a position command of $1.25m$.

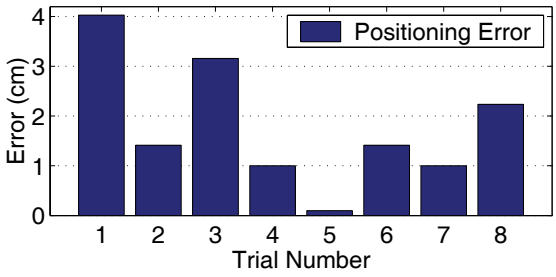

Fig. 15. Final positioning error measured radially from the desired position to the actual crane position.

position command is shown in Fig. 14. This figure depicts motion in the trolley direction only, but each test required the crane to be positioned simultaneously in both the trolley and bridge directions. For the trial depicted in Fig. 14, the trolley started at the $0m$ location and was then commanded to move the the $1.25m$ location. The solid curve represents the position of the trolley throughout the experiment; the dotted curve represents the position of the hook.

The positioning error results for eight trials is shown in Fig. 15. The vertical axis of this figure represents the final radial positioning error between the desired crane position and the actual crane position. Based upon these results, the average radial positioning error is approximately $1.8cm$ with a standard deviation equal to approximately $1.3cm$.

5. CONCLUSIONS

A crane manipulation system (CMS) was developed and implemented on a 30-ton bridge crane. The system is comprised of a machine vision system for sensing hook position, laser range sensors for obtaining bridge and trolley positions, a joystick interface for simplifying gross motion tasks, a visual touchscreen interface for simplifying positioning tasks, and an anti-sway/positioning control

law. The CMS enables operators to manipulate the crane in a nearly swing-free manner. Motion-induced oscillations of the hook were reduced by roughly 90%. The control can also reject externally-induced hook swing. Precision positioning of the hook was demonstrated with positioning capability on the order of a few centimeters.

ACKNOWLEDGEMENTS

This project would not have been possible without the generous support of CAMotion Inc. and Siemens Energy & Automation. Our gratitude is also extended to Mr. Barry Gardner of Logan Aluminum Inc. who provided expert technical competence and service.

REFERENCES

J. Amat, M. Frigola, and A. Casals. Human robot interaction from visual perception. In *IEEE/RSJ Int. Conf. on Intelligent Robots and Systems*, pages 1997–2002, Sendal, Japan, 2004.

Manel Frigola, Josep Fernandez, and Joan Aranda. Visual human machine interface by gestures. In *IEEE Int. Conf. on Robotics & Automation*, pages 386–391, Taipei, Taiwan, 2003.

J. R. Huey and W. Singhose. Experimental verification of stability analysis of closed-loop input shaping controllers,. In *IEEE/ASME Int. Conf. on Advanced Intelligent Mechatronics*, Monterey, CA, 2005, 2005.

V. Kapila, A. Tzes, and Q. Yan. Closed-loop input shaping for flexible structures using time-delay control. *J. of Dynamic Systems, Measurement, and Control*, 122:454–460, 2000.

Michael Kenison and William Singhose. Concurrent design of input shaping and proportional plus derivative feedback control. *J. of Dynamic Systems, Measurement, and Control*, (September), 2002.

Jason Lawrence, Matthew Falkenberg, and William Singhose. Input shaping for a flexible, nonlinear, one-link robotic arm with backlash. In *Japan-USA Symposium on Flexible Automation*, Denver, Colorado, 2004.

Jason Lawrence, William Singhose, and Keith Hekman. Friction-compensating command shaping for vibration reduction. *J. of Vibration and Acoustics*, 127:307–314, 2005.

Marco Muenchhof and Tarunraj Singh. Concurrent feedforward/feedback controller design using time-delay filters. In *AIAA Guidance, Navigation, and Control Conf.*, Monterey, CA, 2002.

Neil C. Singer and Warren P. Seering. Preshaping command inputs to reduce system vibration. *J. of Dynamic Systems, Measurement, and Control*, 112(March):76–82, 1990.

William Singhose, Dooroo Kim, and Michael Kenison. Input shaping control of double-pendulum bridge crane oscillations. *J. of Dynamic Systems, Measurement, and Control*, In Press.

Otto J. M. Smith. Posicast control of damped oscillatory systems. *Proceedings of the IRE*, 45(September):1249–1255, 1957.

Khalid Sorensen and William Singhose. Oscillatory effects of common hard nonlinearities on systems using two-impulse zv input shaping. In *American Control Conf.*, New York City, NY, 2007.

Khalid L. Sorensen, William E. Singhose, and Stephen Dickerson. A controller enabling precise positioning and sway reduction in bridge and gantry cranes. *Control Engineering Practice*, 15(7):825–837, 2007a.

Khalid L. Sorensen, Joshua B. Spiers, and William E. Singhose. Operational effects of crane interface devices. In *IEEE Conf. on Industrial Electronics and Applications*, Harbin, China, 2007b.

Khalid Lief Sorensen. *A Combined Feedback and Command Shaping Controller for Improving Positioning and Reducing Cable Sway in Cranes*. Masters thesis, Georgia Institute of Technology, 2005.

Ulrich Staehlin and Tarunraj Singh. Design of closed-loop input shaping controllers. In *American Control Conf.*, Denver, CO, 2003.

Johan Stahre. Evaluating human/machine interaction problems in advanced manufacturing. *Computer Integrated Manufacturing Systems*, 8(2):143–150, 1995.

Jurg Suter, Dooroo Kim, William Singhose, Khalid Sorensen, and Urs Glauser. Integrating a wireless touchscreen into a bridge crane control system. In *IEEE/ASME Int. Conf. on Advanced Intelligent Mechatronics*, Zurich, Switzerland, 2007.

K. Zuo, V. Drapeau, and D. Wang. Closed loop shaped-input strategies for flexible robots. *Int. J. of Robotics Research*, 14(5):510–529, 1995.